Available online at www.sciencedirect.com
ScienceDirect
Polymer 48 (2007) 382–392
polymer
www.elsevier.com/locate/polymer

Size distribution and shape of nano-nucleus of polyethylene simultaneously determined by SAXS

Kiyoka Okada [a], Kaori Watanabe [b], Isao Wataoka [b], Akihiko Toda [b], Sono Sasaki [c], Katsuaki Inoue [c], Masamichi Hikosaka [b,*]

[a] *Soft Material Physics Group, Graduate School of Biosphere Science, Hiroshima University, 1-7-1 Kagamiyama, Higashi Hiroshima 739-8521, Japan*
[b] *Soft Material Physics Group, Graduate School of Integrated Arts and Sciences, Hiroshima University, 1-7-1 Kagamiyama, Higashi Hiroshima 739-8521, Japan*
[c] *JASRI/SPring-8, 1-1-1 Kouto, Mikaduki-cho, Sayou-gun Hyogo 679-5198, Japan*

Received 7 September 2006; received in revised form 30 October 2006; accepted 31 October 2006
Available online 27 November 2006

Abstract

Nucleation mechanism of polymers was studied by means of small angle X-ray scattering (SAXS) by improving our two previous studies. The first one showed first direct SAXS observation of nucleation of polyethylene (PE). The second one reported how ''size distribution $f(N,t)$'' of nuclei of nano-meter size (nano-nuclei) evolves with time (t), where N is number of ''repeating unit'' in a nucleus. Unfortunately the $f(N,t)$ was obtained by incorrect analysis of SAXS intensity (I_X), i.e., too simple one-dimensional (1D) nucleus was assumed to analyze the I_X. In this paper, we determined simultaneously correct $f(N,t)$ and ''two-dimensional (2D) shape'' of nano-nucleus. From this it is clarified that nano-nucleus shows significant fluctuation in size and shape and repeats frequent generation and disappearance, which corresponds to the conclusion that the end surface free energy of the nano-nucleus (σ_e(nano)) is 1/5 times as large as that of macroscopic crystal (σ_e(macro)). $f(N,t)$ decreased with increase of N. $f(N,t)$ increased and saturated with increase of t.

Keywords: Nucleation; Size distribution; SAXS

1. Introduction

Crystallization from the melt (or gas) is one of the most popular and well known phenomena in any materials. The early state of crystallization controls significantly structure and physical properties of materials. ''Nucleation'' has been assumed theoretically as the early process of the crystallization by classical nucleation theory (CNT) proposed by Becker and Döring, Turnbull and Fisher and Frenkel in 1930 [1–3], but had not been confirmed experimentally. Amazingly nobody has succeeded to observe directly the nucleation from the melt, because number density of nucleus in nano-order (we will name ''nano-nucleus'') was too small to detect. Recently we succeeded in observing nano-nucleation of polyethylene (PE) directly for the first time by means of small angle X-ray scattering (SAXS) by overcoming above problem [4,5].

Scientific goal of nucleation study is to obtain ''experimental real image'' of nano-nucleation and to propose a correct nucleation theory which can explain the concrete facts. We have to approach the scientific goal, i.e., to solve nucleation mechanism from two different sides. One is experimental side and the other is theoretical side.

The experimental side is to clarify real image of nucleation how size, shape and number of nucleus evolve with increase of crystallization time (t), i.e., to make clear size distribution $f(N,t)$, where N is number of atom, ''particle'' or ''repeating unit'' in a nucleus (hereafter we will simply name ''particle''). It has been impossible to observe $f(N,t)$ directly for long time.

In our previous paper, we tried to obtain $f(N,t)$ of PE by analyzing the scattering intensity (I_X) of SAXS [6].

* Corresponding author. Tel.: +81 82 424 6548; fax: +81 82 421 2652.
E-mail address: hikosaka@hiroshima-u.ac.jp (M. Hikosaka).

0032-3861/$ - see front matter © 2006 Elsevier Ltd. All rights reserved.
doi:10.1016/j.polymer.2006.10.042

Unfortunately the $f(N,t)$ was obtained by incorrect analysis of I_X, i.e., too simple one-dimensional (1D) (very long and thin) nucleus was assumed without determining correct shape of nano-nucleus to have Eqs. (10)–(12) in Ref. [6]. As will be shown in this paper, we have to determine experimentally correct $f(N,t)$ and ''shape'' of nano-nucleus at the same time by analyzing I_X. In this paper, the correct shape of nano-nucleus will be shown to be two-dimensional (2D) one. Therefore it is important unsolved problem to obtain correct $f(N,t)$ and shape of nano-nucleus. Purpose of this paper is to determine correct $f(N,t)$ and shape of nano-nucleus simultaneously by analyzing I_X.

The theoretical side is to build up a ''basic equation'' which can explain the observed $f(N,t)$. CNT proposed a ''fundamental kinetic equation'' as a basic equation of nucleation by using $f(N,t)$ [3]. We found a serious problem that the kinetic equation of CNT does not satisfy fundamental ''mass conservation law'', which means that the kinetic equation cannot be regarded as a basic equation [7,8]. We will show in detail and solve this important problem in our sequential paper.

Any basic equation includes parameters (so called ''kinetic parameters'') that give actual information with respect to nucleus, nucleation and so on as described later. The kinetic parameters should be determined experimentally by corresponding theory. As correct observed $f(N,t)$ had not been obtained experimentally, it is important unsolved problem to obtain correct kinetic parameters of nano-nucleus.

1.1. Direct observation of nano-nucleation

Akpalu and Amis tried to observe nucleation from the melt of linear PE by means of SAXS and wide angle X-ray scattering (WAXS), but they did not detect the nucleation well. They observed onset of lamellar stacking [9]. Wang et al. investigated the early stages of isothermal melt crystallization of isotactic polypropylene (iPP) by means of SAXS, WAXS and light scattering [10]. They showed that volume fraction of nuclei is too small to be detectable by SAXS or WAXS. They also addressed that detection limit of the increase of crystallinity by means of WAXS was much lower than that of SAXS.

We succeeded in observing directly nano-nucleation of PE in 2003 by means of SAXS for the first time by adding ''nucleating agent (NA)'' to sample, by which the $I_X(q,t)$ from nano-nuclei increased as high as 10^4 times [4,5], where q is scattering vector. But we observed nucleation of a fixed size of nucleus with $R_g = 162$ Å, where R_g is radius of gyration [11], since the q was limited into a narrow range, $q = (9-14) \times 10^{-3}$ Å^{-1}. Therefore we could not obtain $f(N,t)$.

1.2. $f(N,t)$ is a key to approach nucleation mechanism

CNT predicted time evolution of $f(N,t)$ numerically using the kinetic equation [12–14]. It is obvious that the observed kinetic parameters of nano-nucleus could not be used in the numerical calculation. Since it was impossible to observe $f(N,t)$ directly, the predicted $f(N,t)$ could not be verified for long time. Therefore it is an important unsolved problem to obtain $f(N,t)$ from direct observation of nano-nucleation.

1.3. Shape of nucleus is related to kinetic parameters

It is reasonable to assume that the shape of nano-nucleus is similar to that of ''critical nucleus'', because the critical nucleus should be typical nano-nuclei. We show how shape of nucleus is related to kinetic parameters as follows.

For the sake of simplicity, we think about the three-dimensional (3D) rectangular parallelepiped nucleus with size of l, m and n, where l, m and n are counted by number of particles. N is given by

$$N = lmn \quad \text{for 3D nucleus.} \tag{1}$$

As we assume that shape of a nucleus is similar to that of critical one,

$$l : m : n = l^* : m^* : n^* \quad \text{for 3D nucleus,} \tag{2}$$

where l^*, m^* and n^* are l, m and n of a critical nuclei, respectively.

It is well known that most nucleation of any materials from the bulky melt is heterogeneous nucleation, i.e., nucleus is formed on heterogeneity or NA [15]. In this case, l^*, m^* and n^* are given by

$$\begin{aligned} &l^* = 4\sigma_e/\Delta g,\ m^* = 2\Delta\sigma/\Delta g \text{ and} \\ &n^* = 4\sigma/\Delta g \quad \text{for 3D nucleus,} \end{aligned} \tag{3}$$

where σ_e, $\Delta\sigma$ and σ are free energy of end surface of nucleus, effective interface free energy between NA and crystal and free energy of side surface of nucleus per one particle, respectively, and Δg is free energy of melt per one particle [15]. Δg is given by

$$\Delta g = \Delta s \Delta T = \left(\Delta h/T_m^0\right)\Delta T \propto \Delta T, \tag{4}$$

where Δs is entropy of melting, ΔT is degree of supercooling, Δh is enthalpy of melting per one particle [15] and T_m^0 is equilibrium melting temperature.

As m^* is given by Eq. (3), m^* becomes less than unity ($m^* \leq 1$) with increase of $\Delta g \propto \Delta T$. In this case we have to change the critical nucleus from 3D to 2D ones. As m^* should be integer, m^* of the 2D nucleus is given by

$$m^* = 1 \quad \text{for 2D critical nucleus.} \tag{5}$$

Thus it is summarized to

$$\begin{aligned} m^* &> 1 \quad \text{for } \Delta g < 2\Delta\sigma \text{ or } \Delta T < \Delta T^\dagger \text{ (3D critical nucleus)} \\ &= 1 \quad \text{for } \Delta g \geq 2\Delta\sigma \text{ or } \Delta T \geq \Delta T^\dagger \text{ (2D critical nucleus),} \end{aligned} \tag{6}$$

where

$$\Delta T^\dagger = 2T_m^0\Delta\sigma/\Delta h \tag{7}$$

from Eqs. (4) and (6).

When $m^* = 1$ (2D critical nucleus), we will assume that m of nano-nucleus is unity, i.e.,

$$m = 1 \quad \text{for } \Delta g \geq 2\Delta\sigma \text{ or } \Delta T \geq \Delta T^{\dagger} \text{ (2D nucleus)}. \tag{8}$$

In this case, Eqs. (1) and (2) are changed to

$$N = ln \quad \text{for 2D nucleus} \tag{9}$$

and

$$l : n = l^* : n^* \quad \text{for 2D nucleus}. \tag{10}$$

1.4. How to determine kinetic parameters and $f(N,t)$ of nano-nucleus

It is well known that CNT regarded that nano-nucleus is in quasi-thermal equilibrium in the steady state and that $f(N,t)$ in the steady state ($f_{st}(N)$) satisfies Boltzmann distribution ($P_B(N)$) for $N < N^*$, where N^* is N of critical nucleus [3,13]. $P_B(N)$ includes kinetic parameters as shown in Section 3.3. Kinetic parameters of nano-nucleus and $f(N,t)$ are simultaneously determined by fitting observed $f_{st}(N)$ with $P_B(N)$ for the range of nano-nucleus, i.e., for $N < N^*$.

1.5. One-dimensional nucleus assumed in our previous paper [6]

We assumed too simple long 1D shape of nano-nucleus in our previous paper [6] by assuming that kinetic parameters, i.e., surface free energies are the same between nano-nuclei and macroscopic crystals (we will name macro-crystals), which is a serious problem in nucleation study as we will show in detail later. As shown in this work, we obtained that σ_e of nano-nucleus (σ_e(nano)) was 1/5 times as large as that of macro-crystal (σ_e(macro)), i.e., $\sigma_e(\text{nano}) \cong (1/5)\sigma_e(\text{macro})$, which means that σ_e(nano) was nearly equal to σ of nano-nucleus σ(nano), i.e., $\sigma_e(\text{nano}) \cong \sigma(\text{nano})$. Therefore the shape of the nano-nucleus should be 2D nucleus. Hence obtained $f(N,t)$ assuming 1D nano-nucleus in our previous paper [6] is incorrect.

1.6. Alternative nucleation study on macro-crystals

Alternative nucleation studies, such as studies on heterogeneous nucleation from the bulky melt [16] or homogeneous nucleation in droplets of the melt [17], have been widely carried out in classical nucleation study by observing macro-crystals by means of optical microscope, because it was difficult to observe nano-nucleus directly.

Kinetic parameters such as σ_e, σ and $\Delta\sigma$ have been obtained by observing macro-crystals so far. σ_e was first obtained from the size dependence of melting temperature (T_m) (Gibbs–Thomson plot) of macro-crystals. Other kinetic parameters σ and $\Delta\sigma$ are obtained by solving the simultaneous equations of the ΔT dependences of nucleation rate (I) and growth rate (V) of macro-crystals [16]. The alternative studies assumed that kinetic parameters are the same between macro-crystals and nano-nuclei. It is an interesting problem whether the assumption is correct or not. In this paper, we will show that the above assumption in the alternative nucleation study is not correct. Therefore CNT should be verified by direct observation on nano-nucleus, not by "alternative" indirect observation on macro-crystals.

1.7. Purpose

Purposes of this work is to obtain correct $f(N,t)$ and shape (i.e., kinetic parameters) of nano-nucleus simultaneously by analyzing $I_X(q,t)$, which clarifies "real image" of nano-nucleation.

2. Experimental

The material used in this study was fully fractionated polyethylene (PE, NIST, SRM1483, $M_n = 32 \times 10^3$, $M_w/M_n = 1.1$). The NA of sodium 2,2′-methylene-bis-(4,6-di-*t*-butylphenylene) phosphate (ADEKA Corp., NA-11SF) was used. Mean lateral size of NA (a_{NA}) observed by scanning electron microscope (SEM) was $a_{NA} = 0.23 \pm 0.12$ μm [27]. As small a_{NA} in nm order was missed during sample preparation, a_{NA} should be much smaller than 0.23 μm, i.e., $a_{NA} < 0.23$ μm. PE mixed with NA was prepared [18], which is named as "PE + NA". We used samples of PE + NA to observe nano-nucleation. Concentration of NA in mixture of PE and NA (C_{NA}) was $C_{NA} = 3$ wt%.

When a_0, b_0 and c_0 are the dimensions of a particle or repeating unit, the actual nucleus dimensions are na_0, mb_0 and lc_0 [15]. In the case of PE, we assumed unit cell structure of nano-nucleus as orthorhombic. Therefore ln plane corresponds to the (110) plane [19] and a_0, b_0 and c_0 are $a_0 = 0.46$ nm, $b_0 = 0.42$ nm [20] and $c_0 = 0.13$ nm [21], respectively. Δg of PE given by Eq. (4) [16,22] is

$$\Delta g = 6.8 \times 10^5 \Delta T \ \text{Jm}^{-3}. \tag{11}$$

The sample was melted at 160 °C for 5 min within a thin evacuated capillary (ϕ 1 mm) and then isothermally crystallized at crystallization temperatures (T_cs), $T_c = 126.5$ and 129.0 °C. As $T_m^0 = 139.5$ °C [23], $\Delta T = 10.5$ and 13.0 K, respectively, where ΔT is defined by $\Delta T \equiv T_m^0 - T_c$.

The SAXS experiment was carried out using synchrotron radiation at beam line, BL40B2 of SPring-8 at Japan Synchrotron Radiation Research Institute (JASRI), Harima and BL10C of Photon Factory at Kou Energy Kasokuki Kenkyu Kikou, Tsukuba. The range of q was $q = (7-214) \times 10^{-3}$ Å^{-1} and wave length (λ) was $\lambda = 1.5$ Å.

3. Analysis

3.1. Extended Guinier plot method

Excess scattering intensity $I_X(q,t)$ is defined by

$$I_X(q,t) \equiv I_{Xobs}(q,t) - I_{Xobs}(q,0), \tag{12}$$

where $I_{Xobs}(q,t)$ is observed scattering intensity [4]. It subtracts all effects of so called background which do not relate to nucleation.

As a nucleus is formed on a NA crystal, the observed size distribution function denoted by $f_{obs}(N,t)$ can be given by convolution of $f_{NA}(N)$*$f(N,t)$, i.e., $f_{obs}(N,t) = f_{NA}(N)$*$f(N,t)$ where $f_{NA}(N)$ is size distribution function of NA crystals. It is well known in mathematics that the Fourier transform of the convolution of two functions equals to that of two functions, that is, $\Im[f_{obs}(N,t)] = \Im[f_{NA}(N)]\Im[f(N,t)]$.

It is to be noted that the $I_X(q,t)$ directly corresponds to the $\Im[f_{obs}(N,t)]$. Since it is obvious that the $f_{NA}(N)$ does not depend on N significantly, as compared with $f(N,t)$, we can simplify it as the first approximation in this study that $\Im[f_{obs}(N,t)] \propto \Im[f(N,t)]$. Therefore we can obtain $f(N,t)$ directly from the analysis of observed $I_X(q,t)$ by applying the following method.

When nano-nuclei are isolated and dispersed uniformly, $I_X(q,t)$ is given by summation of the scattering intensity from isolated nucleus [24], i.e.,

$$I_X(q,t) = \sum_j I_{Xj}(q,N_j,t), \tag{13}$$

where j indicates the different nuclei of size N_j and $I_{Xj}(q,N_j,t)$ does $I_X(q,t)$ from the nuclei of N_j. According to Guinier law, $I_X(q,t)$ is approximated by

$$I_X(q,t) \cong \sum_j I^0_{Xj}\exp\left[-R^2_{gj}q^2/3\right] \quad \text{for } R^2_{gj}q^2/3 < 1, \tag{14}$$

where

$$I^0_{Xj} = \Delta\rho^2 N_j^2 f(N_j,t) \tag{15}$$

and $\Delta\rho$ is difference of mean electron density between the nucleus and the melt. When $\ln I_X(q,t)$ is plotted against q^2, $\ln I_X(q,t)$ is decomposed to straight lines. R_{gj} and I^0_{Xj} are obtained from the slope and intercept of the straight lines, respectively, i.e.,

$$R_{gj} = \left\{3\mathrm{d}\ln I_{Xj}(q,N_j,t)/\mathrm{d}q^2\right\}^{1/2}. \tag{16}$$

We will name this as "extended Guinier plot method".

3.2. How to obtain N and f(N,t)

R_g is defined by

$$R_g^2 \equiv \frac{1}{v}\int \mathbf{r}^2 s(\mathbf{r})\mathrm{d}\mathbf{r}, \tag{17}$$

where v is the volume of a nucleus and $s(\mathbf{r})$ is a shape function [25]. $s(\mathbf{r})$ equals to 1 within a nucleus and 0 within the melt. We have

$$\begin{aligned} R^2_{gj} &= \frac{1}{12}\left\{(l_jc_0)^2+(m_jb_0)^2+(n_ja_0)^2\right\} \quad \text{for 3D nucleus} \\ &= \frac{1}{12}\left\{(l_jc_0)^2+(n_ja_0)^2\right\} \quad \text{for } m_j \ll l_j, n_j \text{ or 2D nucleus.} \end{aligned} \tag{18}$$

In this work Eq. (18) is used, which is different from $R_{gj} = l_jc_0/2\sqrt{3}$ for 1D nucleus in the previous paper [6].

From Eqs. (1–3), (9) and (10),

$$\begin{aligned} N_j &= \left(\sigma\Delta\sigma/2\sigma_e^2\right)l_j^3 \quad \text{for 3D nucleus} \\ &= (\sigma/\sigma_e)l_j^2 \quad \text{for 2D nucleus.} \end{aligned} \tag{19}$$

From Eqs. (18) and (19), we have

$$\begin{aligned} N_j &= \frac{93\sqrt{3}\sigma\sigma_e\Delta\sigma}{\left(4\sigma^2+4\sigma_e^2+\Delta\sigma^2\right)^{3/2}}\left(\frac{R_{gj}}{c_0}\right)^3 \quad \text{for 3D nucleus} \\ &= \frac{12\sigma\sigma_e}{\sigma^2+\sigma_e^2}\left(\frac{R_{gj}}{c_0}\right)^2 \quad \text{for 2D nucleus.} \end{aligned} \tag{20}$$

In this work, we used N_j of 2D nucleus given by Eq. (20). Combination of Eqs. (15) and (20) gives

$$\begin{aligned} f(N_j,t) &= \frac{I^0_{Xj}}{\Delta\rho^2}\frac{\left(4\sigma^2+4\sigma_e^2+\Delta\sigma^2\right)^3}{\left(96\sqrt{3}\sigma\sigma_e\Delta\sigma\right)^2}\left(\frac{c_0}{R_{gj}}\right)^6 \quad \text{for 3D nucleus} \\ &= \frac{I^0_{Xj}}{\Delta\rho^2}\left(\frac{\sigma^2+\sigma_e^2}{12\sigma\sigma_e}\right)^2\left(\frac{c_0}{R_{gj}}\right)^4 \quad \text{for 2D nucleus.} \end{aligned} \tag{21}$$

We assumed $\sigma \ll \sigma_e$ (Table 1) and $n \ll l$, which means "rod" like 1D nucleus in our previous paper [6], since we simply used σ and σ_e of macro-crystals without reason. As is shown in Section 1.5, it will be shown later that the assumption is not correct.

3.3. Simultaneous determination of f(N,t) and kinetic parameters

$f_{st}(N)$ should be in proportion to $P_B(N)$ for $N < N^*$, i.e.,

$$P_B(N) = \exp[-\Delta G(N)/kT] \quad \text{for } N < N^*, \tag{22}$$

where $\Delta G(N)$ is a free energy to form a nucleus and k is a Boltzmann constant. $\Delta G(N)$ is given by

$$\begin{aligned} \Delta G(N) &= -\Delta gN + (108\sigma\sigma_e\Delta\sigma)^{1/3}N^{2/3} \quad \text{for 3D nucleus} \\ &= -(\Delta g - \Delta\sigma)N + 4(\sigma\sigma_e)^{1/2}N^{1/2} \quad \text{for 2D nucleus} \end{aligned} \tag{23}$$

[15,26]. Therefore we can evaluate kinetic parameters of nano-nucleus, σ, σ_e and $\Delta\sigma$, by fitting $P_B(N)$ to observed $f_{st}(N)$ by using the following "iteration method" which is one of the technical methods to determine $f(N,t)$ and shape of nano-nucleus simultaneously (shown in Section 1.4).

Table 1
Kinetic parameters

	$\sigma_e/10^{-3}$ Jm^{-2}	$\Delta\sigma/10^{-3}$ Jm^{-2}	$\sigma/10^{-3}$ Jm^{-2}
Nano-nucleus	18.5	1.0 (NA)	7.3[a]
Macro-crystal[b]	88	0.3 (impurity)	8.3

[a] Ref. [28].
[b] Ref. [16].

Step 1 Start from appropriate set of kinetic parameters and calculate $P_B(N)$ by using Eqs. (22) and (23) and obtain $f_{st}(N)$ by using Eqs. (16) and (21). In this study, we started from kinetic parameters of macro-crystals as listed in Table 1.

Step 2 Compare the obtained $f_{st}(N)$ with $P_B(N)$. Boundary condition is

$$f_{st}(0) = P_B(0). \tag{24}$$

Step 3 From the comparison, assume an improved set of kinetic parameters and calculate $P_B(N)$ and $f_{st}(N)$ again. Return back to Step 2 and trace the loop between Step 3 and Step 2 until the best fitting between $f_{st}(N)$ and $P_B(N)$ is obtained. Thus we could finally determine correct $f_{st}(N)$ and kinetic parameters.

Correct $f(N_j,t)$ could be obtained by substituting the parameters, R_{gj} and I^0_{Xj} to Eq. (21).

3.4. 2D nano-nucleus in polymer nucleation

As we succeeded in observing nano-nucleation directly by SAXS by adding nucleating agent (NA) as shown in Section 1.1 [4,5], nuclei are formed on NA crystals. It is a kind of definition of NA that $\Delta\sigma/\sigma$ is small enough. We found that $\Delta\sigma/\sigma$ of most NAs of polymers satisfies

$$\Delta\sigma/\sigma \leq 1/5 \tag{25}$$

[27]. In this paper, we will show that $\Delta\sigma/\sigma$ of PE is about 1/7 by analyzing $I_X(q,t)$ by applying the iteration method shown in Section 3.3. Here we used σ of paraffin [28] as σ(nano),

$$\sigma(\text{nano}) = 7.3 \times 10^{-3}\ \text{Jm}^{-2} \tag{26}$$

and showed in Table 1, since structure of side surface of nano-nucleus should be similar to that of paraffin (or *n*-alkane). In this case, $\Delta T^{\dagger} \cong 7$ K is obtained by using Eq. (7). As observed $\Delta T = 10.5$ and 13.0 K which satisfies

$$\Delta T > \Delta T^{\dagger}, \tag{27}$$

therefore it will be determined that the shape of nucleus becomes 2D one.

In the case of other polymers such as iPP and so on, usually observed ΔT is much larger than 30 K, $\Delta T > 30$ K which satisfies $\Delta T > \Delta T^{\dagger}$ [27]. Therefore the shape of nucleus becomes 2D one.

4. Results

4.1. Excess scattering intensity $I_X(q,t)$

We obtained plot of $I_X(q,t)$ against q as a parameter of t by using Eq. (12) (Fig. 1). $I_X(q,t)$ increased with increase of t. We also obtained ΔT dependence of $I_X(q,t)$. $I_X(q,t)$ increased slowly with increase of t at small ΔT (Fig. 1a). At large ΔT, $I_X(q,t)$ increased more quickly several tens times than that at small ΔT with increase of t (Fig. 1b).

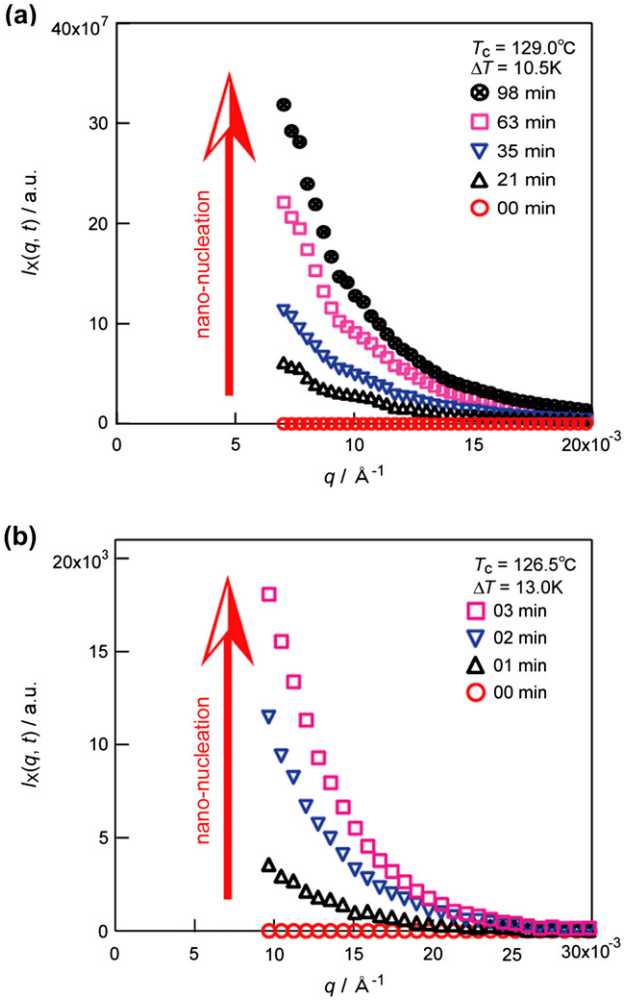

Fig. 1. Degree of supercooling (ΔT) dependence of excess scattering intensity ($I_X(q,t)$) defined by Eq. (12) against scattering vector (q) as a parameter of crystallization time (t). (a) $T_c = 129.0$ °C and $\Delta T = 10.5$ K. (b) $T_c = 126.5$ °C and $\Delta T = 13.0$ K. $I_X(q,t)$ increased with increase of t, which is the evidence of nano-nucleation. Since $I_X(q,t)$ increased slowly with decrease of ΔT, it clarified that nano-nucleation becomes difficult with decrease of ΔT.

In polymer systems, there are many kinds of fluctuations which give SAXS intensity, such as density fluctuation by nucleation, that by spinodal decomposition, density fluctuations in amorphous states, density fluctuations in meso-phase and so on. As only density fluctuation by nucleation changes significantly with decrease of ΔT and finally diminishes at a limit of $\Delta T = 0$, which means $\lim_{\Delta T \to 0} I_X(q,t) = 0$, the observed ΔT dependence of $I_X(q,t)$ clarified that the increase of $I_X(q,t)$ with increase of t is the evidence of nano-nucleation. We will confirm this much more quantitatively in our sequential paper by showing that induction time (τ_i) becomes infinite at a limit of $\Delta T = 0$, i.e., $\lim_{\Delta T \to 0} \tau_i = \infty$. Therefore "induction period" which is named by an early stage of crystallization by CNT is nucleation process and not phase separation such as spinodal decomposition [29].

4.2. Extended Guinier plot method and iteration method

We plotted $\ln I_X(q,t)$ against q^2 as a parameter of t in Fig. 2a. $\ln I_X(q,t)$ increased with increase of t. We applied extended Guinier plot method for $0.05 \times 10^{-3} \leq q^2 \leq 15 \times 10^{-3}$ Å^{-2}. Fig. 2b shows a part of the typical result of extended Guinier plot method for $t = 77$ min. $\ln I_X(q,t)$ was separated into five straight lines of I_{Xj}s by using Eq. (14) for each t. Here I_{X5} which corresponds to the smallest R_{g5} was mainly fitted to the $I_X(q,t)$ for the range of $10 \times 10^{-3} \leq q^2 \leq 15 \times 10^{-3}$ Å^{-2}. We obtained R_{gj} from the slope of the straight lines by using Eq. (16). Slope or R_{gj} increased with decrease of q^2. Vertical intercept $\ln I^0_{Xj}$ was obtained from the straight lines.

The extended Guinier plot method was applied independently for $\ln I_X(q,t)$ vs. q^2 at each observed ts. In order to evaluate the error of obtained R_{gj}s, R_{gj}s were plotted against t in Fig. 3a. All R_{gj}s did not change with increase of t, i.e., it did not depend on t. Thus we obtained time average of R_{gj}s. The relative error (standard deviation) of the R_{gj}s was as small as 3%.

It is to be noted that $I_X(q,t)$ with respect to one size of R_{gj} saturates for lower q since $I_X(q,t)$ becomes Gaussian. In this study, $I_X(q,t)$ of lower q continues to increase until complete solidification because number of larger R_{gj} increases. Although $I_X(q,t)$ at a limit of $q = 0$ should saturate as well known by Ref. [24], it is impossible to observe the saturation for lower q, $q \leq 7 \times 10^{-3}$ Å^{-1} because of limit of resolution.

Fig. 3b shows I^0_{Xj} against t as a parameter of the averaged R_{gj}. I^0_{Xj} started increasing after some onset time and then saturated with increase of t for any R_{gj}, that is the evidence of nano-nucleation. The increase and saturation should correspond to induction and steady periods, respectively. The saturated I^0_{Xj} increased with increase of R_{gj}.

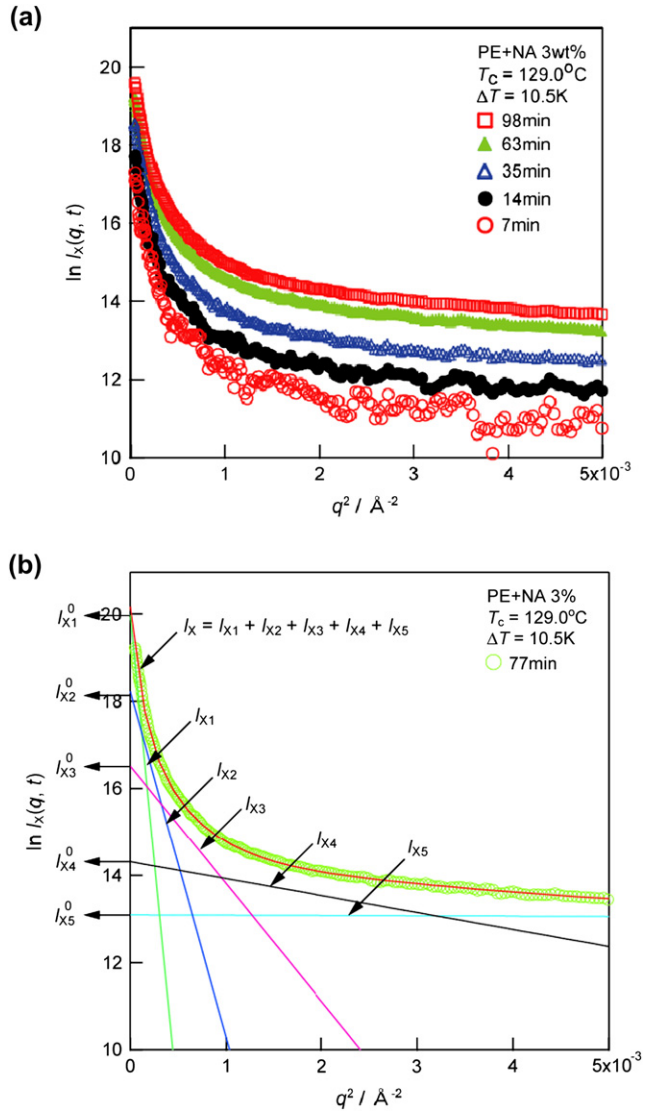

Fig. 2. Plots of $\ln I_X(q,t)$ against q^2. $T_c = 129.0$ °C and $\Delta T = 10.5$ K. (a) $\ln I_X(q,t)$ against q^2 as a parameter of t. (b) Typical result of extended Guinier plot method. Five straight lines (I_{X1}, I_{X2},…I_{X5}) were separated from $\ln I_X(q,t)$ by applying Eq. (14) for $0.05 \times 10^{-3} \leq q^2 \leq 15 \times 10^{-3}$ Å^{-2}. R_{gj} and I^0_{Xj} were obtained from the slope given by Eq. (16) and vertical intercept of the straight lines, respectively, where j indicates the different nuclei of size N_j.

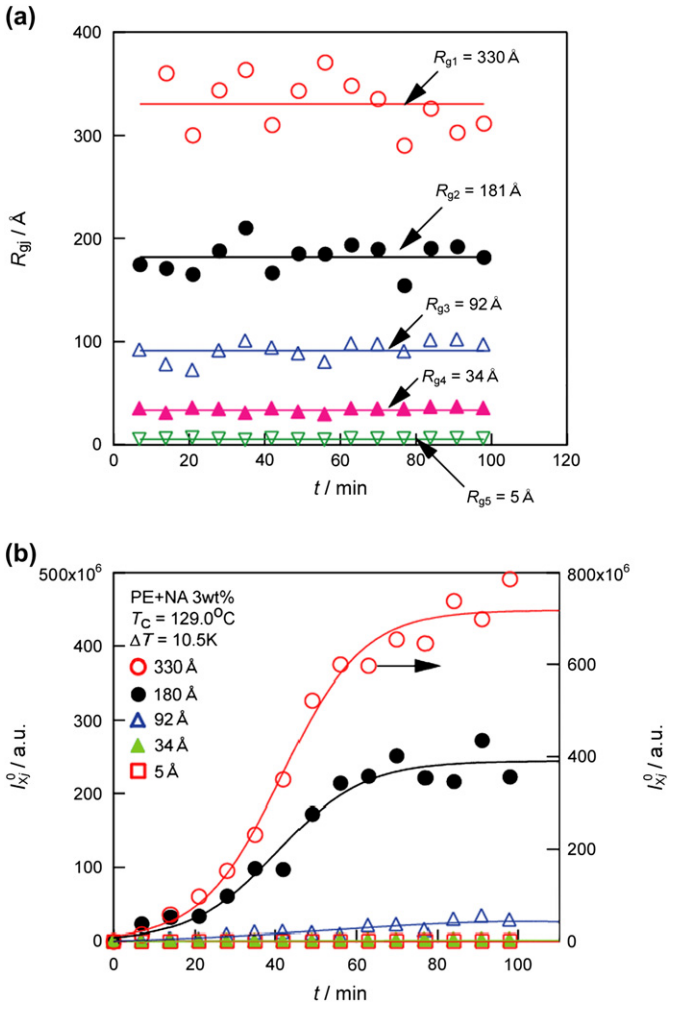

Fig. 3. (a) Plots of R_{gj} against t. Since all R_{gj}s did not depend on t, we obtained time average of R_{gj}s. The relative error of the R_{gj}s was as small as 3%. (b) I^0_{Xj} against t as a parameter of averaged R_{gj}. Right axis indicates I^0_{Xj} of $R_{g1} = 330$ Å and left axis indicates that of the other R_{gj}. I^0_{Xj} increased and saturated with increase of t for any R_{gj}, which is the evidence of nano-nucleation. The increase and saturation should correspond to induction and steady periods, respectively.

4.3. Kinetic parameters and size distribution f(N,t) of nano-nucleus

We determined $f(N,t)$ and shape of nano-nucleus by using iteration method shown in Section 3.3. We obtained kinetic parameters σ_e(nano) and $\Delta\sigma$ of nano-nucleus ($\Delta\sigma$(nano)). They are

$$\sigma_e(\text{nano}) = 18.5 \times 10^{-3}\ \text{Jm}^{-2} \tag{28}$$

and

$$\Delta\sigma(\text{nano}) = 1.0 \times 10^{-3}\ \text{Jm}^{-2}, \tag{29}$$

that are listed in Table 1. In our previous paper [16], $\sigma_e(\text{macro}) = 88 \times 10^{-3}\ \text{Jm}^{-2}$ was obtained (Table 1) using ΔT dependence of I of macro-crystals (Gibbs–Thomson plot) by means of OM [16]. Therefore it is concluded that σ_e(nano) was much smaller than σ_e(macro),

$$\sigma_e(\text{nano}) \cong \frac{1}{5}\sigma_e(\text{macro}) \ll \sigma_e(\text{macro}). \tag{30}$$

We plotted obtained $\log f(N,t)$ against $\log N$ as a parameter of t in Fig. 4. Five plots of $f(N,t)$ in Fig. 4 are ingredients decomposed by Eq. (14). $f(N,t)$ decreased with increase of N for any t. This means that a little part of nano-nuclei survive and grow up to macro-crystals. $f(N,t)$ increased with increase of t at a fixed N and stopped increasing after 10^2 min for $N \leq N^*$. The increase and stop of increase indicate the induction and steady periods, respectively.

4.4. Time evolution of size distribution f(N,t) and induction time τ_i

Fig. 5a shows time evolution of $f(N,t)$ as a parameter of N. $f(N,t)$ of smaller N increased faster significantly and saturated

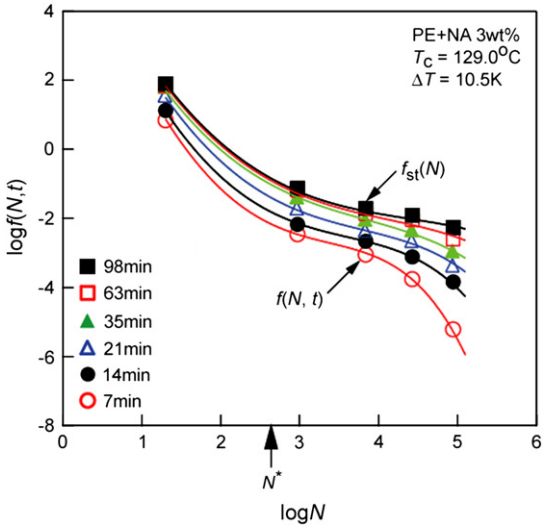

Fig. 4. Plots of size distribution $\log f(N,t)$ against $\log N$ as a parameter of t. Five plots of $f(N,t)$ are ingredients decomposed by Eq. (14). N of critical nucleus (N^*) was $N^* \cong 450$ repeating unit. $f_{st}(N)$ is $f(N,t)$ in the steady state for $N < N^*$. $f(N,t)$ decreased with increase of N for any t. This means that a little part of nano-nuclei survive and grow up to macro-crystals.

with increase of t. $f(N,t)$ of larger N increased much slower and saturated with increase of t. We showed τ_i after definition of Andres and Boudart [30]. We made clear real image of nano-nucleation for the first time in Fig. 5b. At first, smaller nano-nuclei generated for $t = 7$ min. A lot of nano-nuclei generated and a part of them grew up to larger one for $t = 35$ min. Much more nano-nuclei and larger one generated and grew up for $t \cong 100$ min. It clarified that probability of nucleation on NA (P_{NA}) was $P_{NA} \ll 1$, i.e., heterogeneous nucleation is probabilistic phenomenon since $f(N,t)$ saturated as shown later [18]. Probabilistic phenomenon means that nucleation mechanism does not be interacted by NA. If nucleation is not probabilistic, P_{NA} will be $P_{NA} \cong 1$.

We plotted τ_i against $\log N$ (Fig. 6). τ_i increased with increase of N. Experimental formula was given by

$$\tau_i \propto \log N. \tag{31}$$

It is interesting to observe nano-nucleation by other methods like WAXS, differential scanning calorimeter (DSC), infrared ray (IR) and so on, which is next problem.

4.5. Size distribution in steady state $f_{st}(N)$ and Boltzmann distribution $P_B(N)$

The obtained $f_{st}(N)$ in Fig. 4 against N is fitted with $P_B(N)$ of this work (P_B(nano)) for $N < N^*$ using a boundary condition of Eq. (24), which is shown in Fig. 7a. P_B(nano) fitted the $f_{st}(N)$ very well for $N < N^*$. For comparison, $P_B(N)$ of macro-crystals (P_B(macro)) is also shown in Fig. 7a using kinetic parameters of macro-crystals (Table 1) using the same boundary condition. P_B(macro) did not fit $f_{st}(N)$ at all for $N < N^*$.

If nano-nucleation is thermal equilibrium phenomenon for all N, $f_{st}(N)$ should satisfy Boltzmann distribution. Hence $f_{st}(N)$ should have a minimum at $N = N^*$ and increase significantly for $N > N^*$. But observed $f_{st}(N)$ decreases with increase of N. Therefore P_B(nano) does not fit for $N > N^*$ at all. This is an important mystery, which means the nucleation in $N > N^*$ should be a kind of nonequilibrium kinetic phenomenon. We will explain this mystery by proposing a new nucleation theory which will be shown in our sequential paper.

5. Discussion

5.1. Probability of nucleation on NA (P_{NA})

It is shown in CNT that when probability of nucleation of NA (P_{NA}) is large (i.e., $P_{NA} \cong 1$), the $f(N,t)$ for small N should show a maximum and then decrease as schematically shown in Fig. 5c [31]. Therefore the above result that $f(N,t)$ saturates and does not show any maximum indicates that

$$P_{NA} \ll 1. \tag{32}$$

This means that nuclei generate statistically on numerous NAs, that is, the present heterogeneous nucleation is a kind of statistical process similar to the homogeneous nucleation.

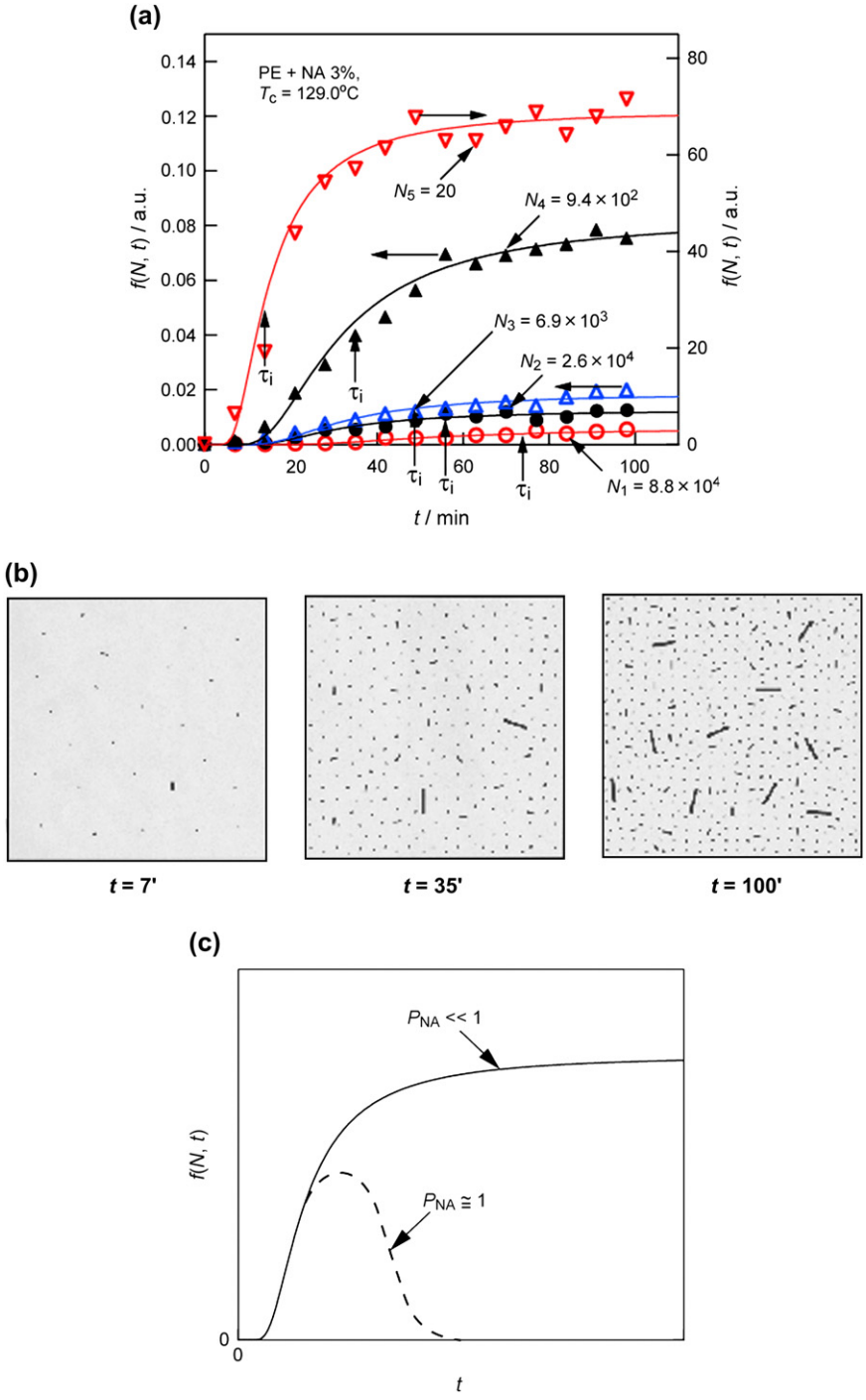

Fig. 5. Time evolution of $f(N,t)$ which clarifies "real image" of nano-nucleation. (a) Time evolution of $f(N,t)$ as a parameter of N. Right axis indicates $f(N,t)$ of $N_5 = 20$ repeating unit and left axis indicates that of the other N_j. $f(N,t)$ of smaller N increased faster significantly and saturated with increase of t. Induction times (τ_is) were shown after definition of Andres and Boudart [30]. (b) Illustration of "real image" of nano-nucleation. Smaller nano-nuclei generated for $t = 7$ min. A lot of nano-nuclei generated and a part of them grew up to larger one for $t = 35$ min. Much more nano-nuclei and larger one generated and grew up for $t \cong 100$ min. (c) Schematic illustration of difference of time evolution of $f(N,t)$ by probability of nucleation on NA (P_{NA}). When $P_{NA} \cong 1$, $f(N,t)$ should show a maximum and then decrease. Since obtained $f(N,t)$ saturated and does not show any maximum, $P_{NA} \ll 1$. This means that nuclei generate statistically on numerous NAs.

5.2. Real image of nano-nucleation

As $\sigma_e(\text{nano}) \ll \sigma_e(\text{macro})$ was shown in Eq. (30), we have

$$\Delta G_{\text{nano}}(N) \ll \Delta G_{\text{macro}}(N) \quad \text{for } N \leq N^*, \tag{33}$$

where $\Delta G_{\text{nano}}(N)$ and $\Delta G_{\text{macro}}(N)$ are $\Delta G(N)$ calculated using $\sigma_e(\text{nano})$ and $\sigma_e(\text{macro})$ in Eq. (23), respectively. Fig. 7b shows plots of $\Delta G_{\text{nano}}(N)$ and $\Delta G_{\text{macro}}(N)$. We have in the present study by using Eq. (23),

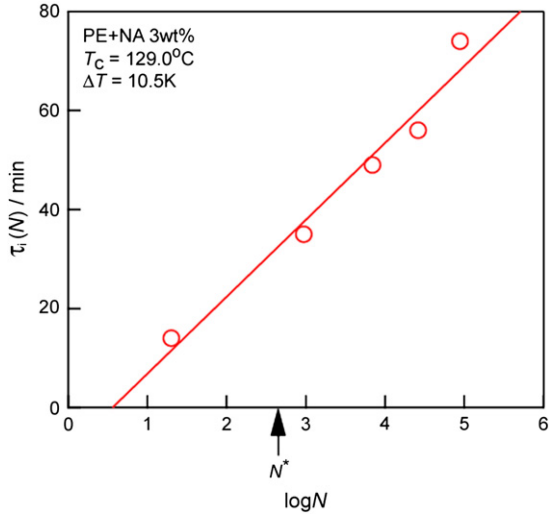

Fig. 6. Plots of τ_i against $\log N$. $T_c = 129.0\ ^\circ\mathrm{C}$ and $\Delta T = 10.5$ K. τ_i increased with increase of N.

$$\Delta G^*_{\mathrm{nano}}\left(N^*_{\mathrm{nano}}\right) \cong 10kT \ll \Delta G^*_{\mathrm{macro}}\left(N^*_{\mathrm{macro}}\right) \cong 33kT \quad \text{for } \Delta T = 10.5\ \mathrm{K}, \tag{34}$$

where $\Delta G^*_{\mathrm{nano}}$, $\Delta G^*_{\mathrm{macro}}$, N^*_{nano} and N^*_{macro} are ΔG^* and N^* calculated using σ_e(nano) and σ_e(macro), respectively. In this case,

$$N^*_{\mathrm{nano}} \ll N^*_{\mathrm{macro}} \tag{35}$$

is also obtained. From the above considerations, the fluctuation of nano-nucleus with respect to the shape and/or size is very large (Fig. 8). Hence nano-nucleus can take all possible shapes and has large entropy. Nano-nucleus should be generated and disappeared frequently. In particular, attachment and detachment of particles are very frequent on the interface of nucleus and there is significant unevenness. Therefore it is natural that nano-nucleus is in quasi-thermal equilibrium state. We clarified the real image of nano-nucleus for the first time.

On the other hand, macro-crystal has less fluctuation with respect to its shape and size in Fig. 8. Actually we can neglect the disappearance of crystal and $f(N,t)$ cannot decrease with increase of N for $N \gg N^*$, as optical observation usually shows. Therefore P_B(macro) cannot fit. In the case of macro-crystals, it is well known that surface particles are thermodynamically reconstructed into smooth and flat surface by surface diffusion, which is a kind of "Ostwald ripening" and results in large σ_e(macro).

5.3. End surface of polymer crystals

It is interesting to clarify what kind of molecular structure of end surface of polymer crystals corresponds to small and large σ_es of nano-nucleus and macro-crystal of polymers, respectively. Fig. 9 shows that nano-nucleus will form loose fold or bundle nucleus as Price predicted [15]. In the case of loose fold or bundle type nano-nucleus (small N), chain density on the end surface is small and not overcrowded. In the case of fold type nano-nucleus, on the other hand, energy to form sharp folds is very large because one fold has to have three Gauche in the case of PE [19]. Therefore σ_e(loose fold or bundle) is much smaller than σ_e(fold), i.e.,

$$\sigma_e(\text{loose fold or bundle}) \ll \sigma_e(\text{fold}) \quad \text{for small } N. \tag{36}$$

Macro-crystals tend to form sharp fold [32]. If nucleus keeps bundle all the way, chain density of end surface increases with increase of N. So macro-crystal forms fold to protect overcrowded state of chains. We think that it is advantageous for macro-crystals. Energy to form fold will become smaller than that to form bundle or loose fold. Therefore it is expected that

$$\sigma_e(\text{loose fold or bundle}) \gg \sigma_e(\text{fold}) \quad \text{for large } N. \tag{37}$$

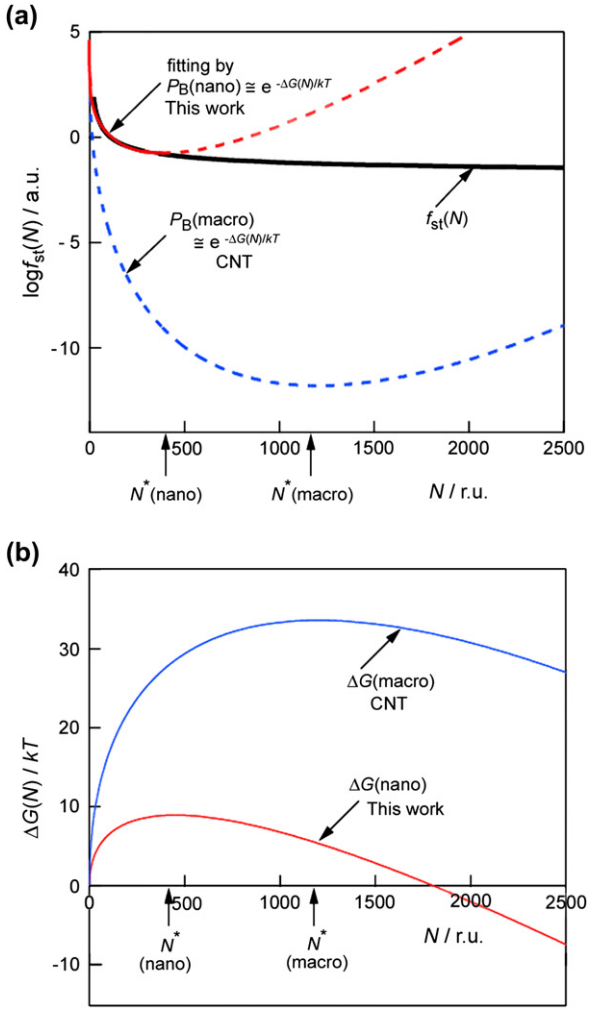

Fig. 7. (a) Fitting of obtained $\log f_{st}(N)$ with P_B(nano) and P_B(macro). The Boltzmann distribution P_B(nano) and P_B(macro) were calculated by using kinetic parameters of nano-nucleus and macro-crystal, respectively (Table 1). The P_B(nano) fitted the $f_{st}(N)$ very well for $N < N^*$, but the P_B(macro) did not fit at all. (b) Free energy to form a nucleus $\Delta G(N)$ against N of nano-nucleus and macro-crystal which correspond to P_B(nano) and P_B(macro) of (a), respectively. $\Delta G_{\mathrm{nano}}(N)$, $\Delta G_{\mathrm{macro}}(N)$, N^*_{nano} and N^*_{macro} are $\Delta G(N)$ and N of critical nucleus calculated using σ_e(nano) and σ_e(macro) in Eq. (23), respectively. $\Delta G_{\mathrm{nano}}(N)$ was much smaller than $\Delta G_{\mathrm{macro}}(N)$, $\Delta G_{\mathrm{nano}}(N) \ll \Delta G_{\mathrm{macro}}(N)$ for $N \leq N^*$.

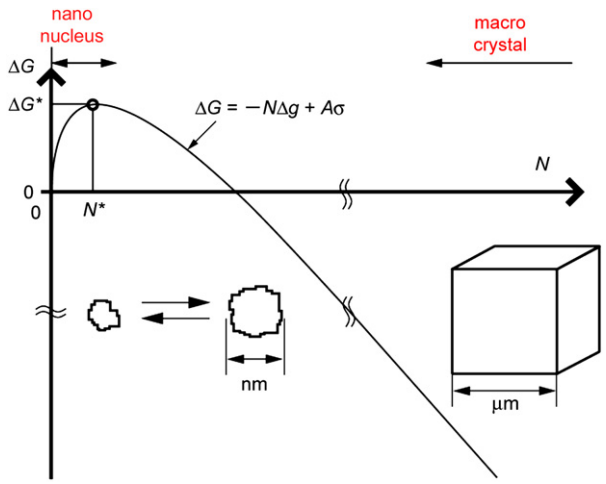

Fig. 8. Illustration of ΔG(N), nano-nucleus and macro-crystal. The fluctuation of nano-nucleus with respect to the shape and/or size is very large, which clarified the ''real image'' of nano-nucleation for the first time. Macro-crystal has less fluctuation with respect to its shape and size. It is well known that surface particles are reconstructed into rather smooth and flat surface by surface diffusion which is a kind of ''Ostwald ripening''.

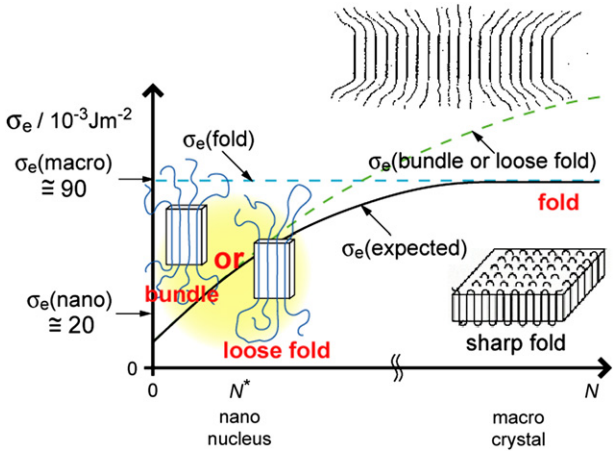

Fig. 9. Schematic illustration of σ_e against N. Nano-nucleus should form loose fold or bundle nucleus as Price predicted [15] because energy to form sharp folds is very large. Macro-crystal tends to form sharp fold [32]. Therefore σ_e(expected) shows the size dependence of expected σ_e.

We show the size dependence of expected σ_e as σ_e(expected) in Fig. 9. It is concluded that molecular structure of end surface, i.e., σ_e changes with increase of N.

6. Conclusion

We observed small angle X-ray scattering (SAXS) intensity $I_X(q,t)$ of nano-nucleation directly for wide range of scattering vector (q), $q = (7-214) \times 10^{-3}$ Å^{-1}. Correct size distribution $f(N,t)$ and two-dimensional (2D) shape (i.e., kinetic parameters) of nano-nucleus were obtained simultaneously for the first time by analyzing $I_X(q,t)$ using extended Guinier plot method. Here N is number of ''particle'' and t is crystallization time. $f(N,t)$ decreased with increase of N for each t. $f(N,t)$ increased with increase of t and saturated for each N.

We found that the free energy of end surface (σ_e) of nano-nucleus (σ_e(nano)) is much smaller than that of macro-crystal (σ_e(macro)), i.e., σ_e(nano) ≅ 1/5σ_e(macro). Therefore it is concluded that nano-nucleus shows significant fluctuation with respect to size and shape and repeats frequent generation and disappearance, by which ''real image'' of nano-nucleation was clarified. In the case of macro-crystals, it is well known that surface particles are thermodynamically reconstructed into smooth and flat surface by surface diffusion, which is a kind of ''Ostwald ripening'' and results in large σ_e(macro).

Acknowledgements

The authors are grateful to ADEKA Corp. for supplying the nucleating agent, NA-11SF. The authors also thank to Dr. Shinichi Yamazaki of Okayama University and Dr. Narayan Ch. Das and Dr. Motoi Yamashita of Hiroshima University, for their kind help. The synchrotron radiation experiments were performed at the BL40B2 in the SPring-8 with the approval of the Japan Synchrotron Radiation Research Institute (JASRI) (Proposal No. 2004B0271-NL2b-np, No. 2006A1576) and at the BL10C in the Photon Factory (PF) with the approval of the Kou Energy Kasokuki Kenkyu Kikou (KEK) (Proposal No. 04G069).

References

[1] Becker VR, Döring W. Ann Phys 1935;24:719–52.
[2] Turnbull D, Fisher JC. J Chem Phys 1949;17:71–3.
[3] Frenkel J. Kinetic theory of liquids. New York: Dover Publications, Inc.; 1946.
[4] Hikosaka M, Yamazaki S, Wataoka I, Das NC, Okada K, Toda A, et al. J Macromol Sci Phys 2003;B42:847–65.
[5] Hikosaka M, Watanabe K, Okada K, Yamazaki S. Adv Polym Sci 2005; 191:137–86.
[6] Das NC, Hikosaka M, Okada K, Toda A, Inoue K. J Chem Phys 2005; 123:204906/1–5.
[7] Hikosaka M, Okada K, Watanabe K, Toda A. Polym Prepr Jpn 2005; 54(2):3073–4.
[8] Hikosaka M, Okada K, Watanabe K, Toda A, Sasaki S. Polym Prepr Jpn 2006;55(2):3087–8.
[9] Akpalu YA, Amis EJ. J Chem Phys 1999;111:8686–95.
[10] Wang ZG, Hsiao BS, Sirota EB, Agarwal P, Srinivas S. Macromolecules 2000;33:978–89.
[11] Tanaka H. Koubunshi no butsurigaku. 3rd ed. Tokyo: Syoukabou; 2001 [chapter 2].
[12] Auer S, Frenkel D. Nature 2001;409:1020–3.
[13] Kelton KF, Greer AL, Thompson CV. J Chem Phys 1983;79(12): 6261–76.
[14] Demo P, Kozisek Z. Phys Rev B 1993;48(6):3620–5.
[15] Price FP. In: Zettlemoyer AC, editor. Nucleation. New York: Marcel Dekker; 1969. p. 405–88.
[16] Ghosh SK, Hikosaka M, Toda A, Yamazaki S, Yamada K. Macromolecules 2002;35(18):6985–91.
[17] Cormia RL, Price FP, Turnbull D. J Chem Phys 1962;37(6):1333–40.
[18] Okada K, Watanabe K, Urushihara T, Toda A, Hikosaka M. Polymer, in press. doi:10.1016/j.polymer.2006.10.048.
[19] Corradini P, Petraccone V, Asslegra G. Macromolecules 1971;4(6):770–1.
[20] Hoffman JD, Frolen LJ. J Res Natl Bur Stand 1975;79A(6):671–99.

[21] Tadokoro H. Structure of crystalline polymers. New York: A Wiley-Interscience Publication; 1979. p. 353–75.
[22] Hikosaka M. Polymer 1987;28:1257–64.
[23] Okada M, Mishi M, Takahashi M, Matsuda H, Toda A, Hikosaka M. Polymer 1998;39:4535–9.
[24] Ottani S, Ferracini E, Ferrero A, Malta V, Porter RS. Macromolecules 1995;28:2411–23.
[25] Guinier A. Theory of technique of the radiocrystallography. Japanese ed. Tokyo: Rigaku Denki; 1967.
[26] Binsbergen FL. J Polym Sci 1973;11:117–35.
[27] Urushihara T, Okada K, Watanabe K, Toda A, Tobita E, Kawamoto N, et al. Polym J 2007;39(1).
[28] Sato K, Kobayashi M. Shishitsu no Kouzou to Dynamics. Tokyo: Kyouritsu Syuppann; 1992 [chapter 7].
[29] Imai M, Mori K, Kizukami T, Kaji K, Kanaya T. Polymer 1992;33: 4457–62.
[30] Andres RP, Boudart M. J Chem Phys 1965;42(6):2057–64.
[31] Kozisek Z, Hikosaka M, Demo P, Sveshnikov AM. J Cryst Growth 2005;275:e79–83.
[32] Keller A. Philos Mag 1957;2:1171–5.